Available online at www.sciencedirect.com
ScienceDirect
Biochimica et Biophysica Acta 1768 (2007) 2831–2840
Biochimica et Biophysica Acta BBA
www.elsevier.com/locate/bbamem

A multidomain outer membrane protein from *Pasteurella multocida*: Modelling and simulation studies of PmOmpA

Timothy Carpenter [1], Syma Khalid [1], Mark S.P. Sansom *

Department of Biochemistry, University of Oxford, South Parks Road, Oxford, OX1 3QU, UK

Received 7 May 2007; received in revised form 6 July 2007; accepted 26 July 2007
Available online 16 August 2007

Abstract

PmOmpA is a two-domain outer membrane protein from *Pasteurella multocida*. The N-terminal domain of PmOmpA is a homologue of the transmembrane β-barrel domain of OmpA from *Escherichia coli*, whilst the C-terminal domain of PmOmpA is a homologue of the extra-membrane *Neisseria meningitidis* RmpM C-terminal domain. This enables a model of a complete two domain PmOmpA to be constructed and its conformational dynamics explored via MD simulations of the protein embedded within two different phospholipid bilayers (DMPC and DMPE). The conformational stability of the transmembrane β-barrel is similar to that of a homology model of OprF from *Pseudomonas aeruginosa* in bilayer simulations. There is a degree of water penetration into the interior of the β-barrel, suggestive of a possible transmembrane pore. Although the PmOmpA model is stable over 20 ns simulations, retaining its secondary structure and fold integrity throughout, substantial flexibility is observed in a short linker region between the N- and the C-terminal domains. At low ionic strength, the C-terminal domain moves to interact electrostatically with the lipid bilayer headgroups. This study demonstrates that computational approaches may be applied to more complex, multi-domain outer membrane proteins, rather than just to transmembrane β-barrels, opening the possibility of *in silico* proteomics approaches to such proteins.

Keywords: Outer membrane protein; OmpA; Molecular dynamics; Homology model; RmpM; OprF

1. Introduction

Outer membrane proteins (OMPs) span the outer membrane of Gram-negative bacteria, extending at one end into the extracellular environment and the other into the periplasmic space. OMPs are also found in the cell envelopes of certain Gram-positive bacteria, and in the outer membrane of mitochondria. It has been predicted that OMPs constitute 2–3% of the Gram-negative bacterial genome [1,2]. OMPs are of interest from a biomedical perspective as potential targets for novel antimicrobial drugs and vaccines [3,4]. The generic structure of the OMP family is an anti-parallel β-sheet that forms a β-barrel structure [5]. The OMPs cover a number of different functions [6] including multimeric porins (e.g. OmpF and PhoE [7]), complex transport proteins (e.g. FhuA [8]), simple OMPS (e.g. OmpA [9]), as well as enzymes such as OmpT [9] and PagP [10,11] and recognition proteins (e.g. OpcA [12]).

Perhaps the simplest class of OMPs is exemplified by OmpA, which is the major OMP of the *Escherichia coli* outer membrane [13] and plays a key role in biofilm formation [14]. OmpA is composed of an N-terminal domain (residues 1 to 171) which forms an 8-stranded anti-parallel transmembrane (TM) β-barrel, and a C-terminal domain (residues 172 to 325). The latter is homologous to an OmpA-like C-terminal domain of RmpM from *Neisseria meningitidis*, the structure of which has been determined [15] and which is thought to interact with periplasmic peptidoglycan. A flexible proline-rich sequence links the two domains. The N-terminal domain structure of OmpA has been determined both by protein crystallography and NMR [9,16].

PmOmpA is the major protein of the outer membranes of *Pasteurella multocida*. It has been shown that PmOmpA plays a role in the interaction of *P. multocida* with extracellular matrix molecules [17]. Structural and functional characterisations of

* Corresponding author. Tel.: +44 1865 275371; fax: +44 1865 275273.
E-mail address: mark.sansom@bioch.ox.ac.uk (M.S.P. Sansom).
[1] These authors contributed equally to this paper.

0005-2736/$ - see front matter © 2007 Elsevier B.V. All rights reserved.
doi:10.1016/j.bbamem.2007.07.025

PmOmpA have also suggested a possible role for this protein in *P. multocida* — host relationships and therefore in the pathogenesis of *P. multocida*. Furthermore it has been shown that pre-binding of anti-PmOmpA antibodies to these proteins decreases their binding to the matrix molecules [17]. An important step in gaining insights into the mechanism of adherence would be to characterise the structure and dynamics of PmOmpA. However it is difficult to conduct such a study using experimental methods alone, not least because of the sparse structural data available for OMPs. Indeed the role of OMPs in the pathogenic action of bacteria is still not well understood due to lack of key structural data. Recently homology modelling and molecular simulations have successfully been applied to OprF, an OMP from *Pseudomonas aeruginosa* [18], and to the transferrin-binding protein A from *N. meningitides* [19]. PmOmpA is an ideal case for such a study; the N-terminal domain shares a 40% identity with *E. coli* OmpA (henceforth EcOmpA), whose structure is known, and the C-terminal domain shares a 40% sequence identity with the *N. meningitidis* RmpM C-terminal domain, whose structure is also known. A short (relative to the ~18 residue linker of EcOmpA), 4-residue linker connects the two domains.

In this paper we present modelling and simulation studies of both the N-terminal domain of PmOmpA and of the intact protein, both in the presence of a phospholipid bilayer. These studies provide an evaluation of the use of homology modelling and simulations to explore multi-domain OMPs, in contrast to previous studies which have focused on the TM domains [20–23]. The simulations of the intact PmOmpA model suggest a role for electrostatics in mediating interactions between the C-terminal domain and the periplasmic surface of the membrane.

2. Methods

2.1. PmOmpA models

PmOmpA models were based on sequence alignments obtained using ClustalW 1.83 (http://www.ebi.ac.uk/clustalw/) [24,25], including gap-penalties. The N-terminal domain model was generated from the OmpA N-terminal domain structure (PDB code 1BXW), while the RmpM C-terminal domain (PDB code 1R1M) was used as a template for the C-terminal domain. Models were built using Modeller 4.10 (http://salilab.org/modeller/) [26,27] and their stereochemistry evaluated using PROCHECK [28]. The linker region, of only four amino acids, was modelled firstly by adding the linker sequence to the N-terminal structure, and also by treating the linker sequence as an extension of the C-terminal structure. Thus two ensembles of linker structures were created as extensions, one ensemble from each template. Analysis of the two ensembles revealed the linker conformations with the lowest energies to be similar (RMSD of only 0.40 Å). The linker model with the lowest energy overall was from the ensemble modelled as an extension of the C-terminal domain. The most suitable C-terminal model, identified using PROCHECK, with the linker region present was manually docked onto the N-terminal domain model. The model of the intact protein was then subjected to energy minimisation to optimise the geometry of the linker.

2.2. Simulation system setup

The simulation protocol was similar to that used in previous studies of OmpA and related proteins[18,29,30]. The PmOmpA models were embedded in a pre-equilibrated dimyristoylphospatidylcholine (DMPC) bilayer. The protein was oriented with its principal axis perpendicular to the bilayer normal. The bands of aromatic residues on the surface of the N-terminal domain were used to position the β-barrel in the lipid bilayer. Neutralising chloride ions were added by replacing randomly chosen water molecules. The equilibration stage of energy minimisation and 0.5 ns of protein-restrained dynamics was followed by a unrestrained MD run on a multi-nanosecond timescale.

2.3. Simulation protocol

All simulations were performed using the GROMACS 3.14 simulation package (www.gromacs.org) [31] with an extended united atom version of the GROMOS96 force field [32]. All energy minimisations used <1000 steps of steepest descents to relax any steric conflicts generated during setup. During restrained runs all protein non-hydrogen atoms were harmonically restrained with a force constant of 1000 kJ mol^{-1} nm^{-2}. Long-range electrostatic interactions were treated using the particle mesh Ewald method [33] with a 1-nm

Table 1
Summary of simulations

Simulation	Model [a]	Lipid	Ionic strength [b]	Duration (ns)		Cα RMSF [c] (Å)	Cα RMSD [d] (Å)
Sim1	Barrel model	DMPC	Low	15		1.1	3.3
Sim2	Barrel model	DMPC	1 M	10		0.9	2.2
Sim3	Barrel model uncharged	DMPC	Low	10		1.4	3.3
Sim4	Barrel model R156G	DMPC	Low	10		1.2	3.3
Sim5	Intact protein	DMPC	Low	20	All	3.8	10.4
					N	1.0	2.4
					C	1.4	2.9
Sim6	Intact protein	DMPC	1 M	20	All	2.8	6.5
					N	1.0	2.4
					C	1.3	4.2
Sim7 [e]	Intact protein	DMPE	Low	25	All	3.4	6.5
					N	0.9	1.9
					C	1.4	2.8
Sim8 [e]	Intact protein	DMPE	Low	20	All	1.5	4.0
					N	0.9	1.7
					C	1.1	2.2

[a] Simulations Sim1 to Sim4 are for the N-terminal β-barrel TM domain only; simulations Sim5 and Sim6 are for the intact protein, i.e. the N-terminal and C-terminal domains. For the latter two simulations RMSF and RMSD values are reported for the intact protein ("all") and for the N- and C-terminal domains respectively.

[b] Two different protocols were used for the solution bathing the membrane: either sufficient counterions were added to neutralise the charge on the protein ("low"), or Na^+ and Cl^- ions were added equivalent to a final concentration of ~1 M.

[c] RMSFs of Cα atoms were evaluated relative to average positions over the duration of each simulation.

[d] The values of the Cα RMSDs relative to the starting model are the plateau values for each simulation.

[e] The RMSD values for these simulations were carried out with respect to the start frame of the simulation, i.e. t=6 ns from Sim5 for Sim7 and t=20 ns from Sim5 for Sim8.

cutoff for the real space calculation. A 1-nm cutoff was used for the van der Waals interactions. All simulations were performed in the constant number of particles, pressure and temperature (*NPT*) ensemble. The temperature of the protein, lipids, water and ions was coupled separately using the Berendsen thermostat [34] at 310 K with a coupling constant τ_T=0.5 ps. The pressure was coupled semi-isotropically using the Parrinello–Rahman barostat [35] at 1 bar with coupling constant τ_P=1 ps. The timestep for integration was 2 fs. The LINCS algorithm [36] was used to restrain bond lengths.

2.4. General analysis

Analyses were performed using GROMACS routines and locally written scripts. Secondary structure analyses used DSSP [37]. Pore-like regions within the barrel interior were analysed and visualised using HOLE [38]. Molecular graphics images were generated using VMD [39] and Rasmol as implemented within Rastop (http://www.geneinfinity.org/rastop).

3. Results

Three sets of simulations were performed. The first (Sim1 to Sim4; see Table 1) was of the N-terminal β-barrel domain, embedded in a dimyristoyl phosphatidylcholine (DMPC) bilayer. The second set (Sim5 and Sim6) was of the intact PmOmpA protein again embedded in a DMPC bilayer (Fig. 1) whilst the third set (Sim7 and Sim8) was of the intact PmOmpA embedded in a dimyristoyl phosphatidylethanolamine (DMPE) lipid bilayer.

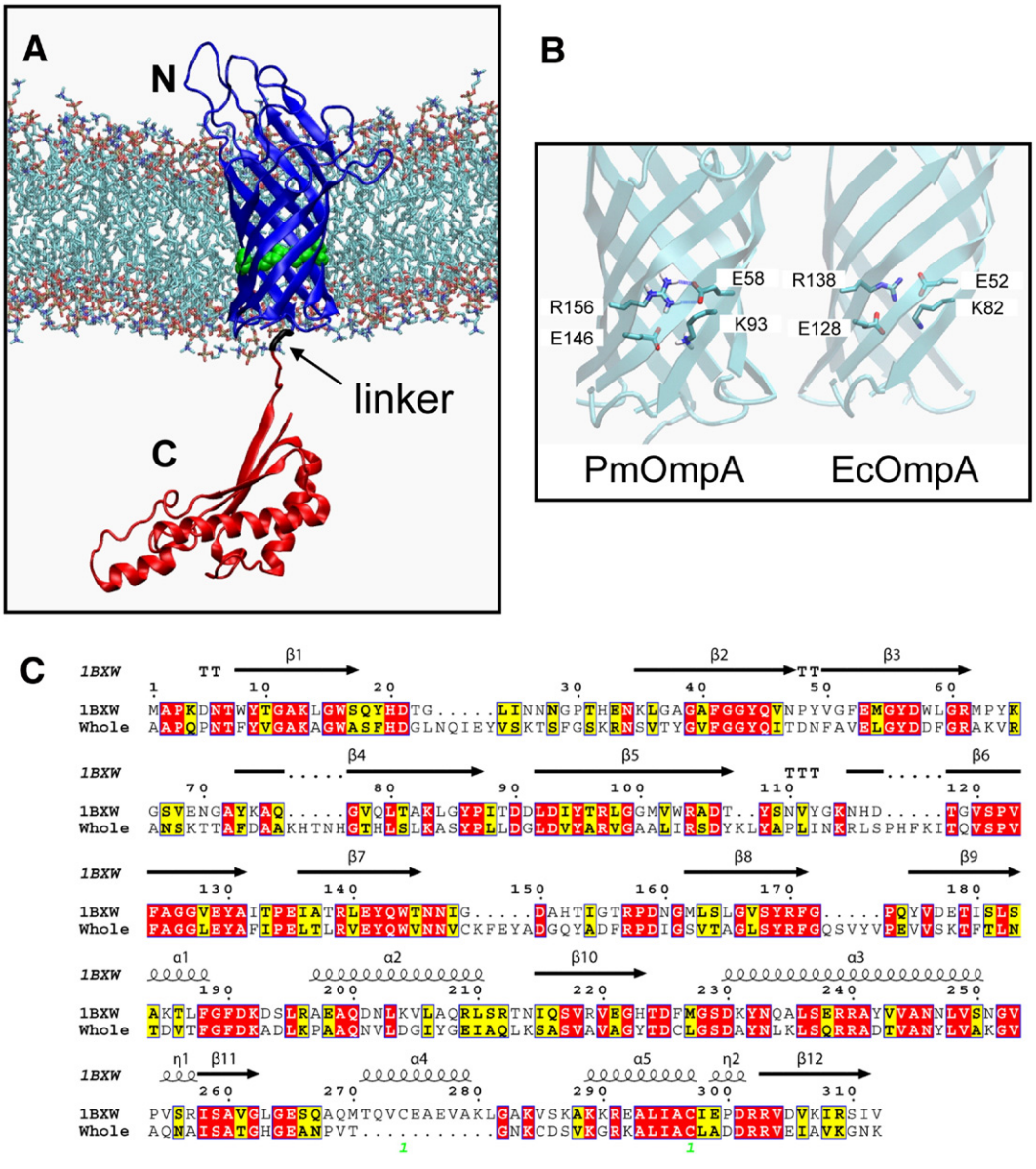

Fig. 1. (A) Model of the intact PmOmpA protein in a DMPC bilayer (as in simulations Sim5 and Sim6). The N-terminal β-barrel domain (blue) spans the lipid bilayer whilst the C-terminal domain (red) sits in the periplasmic region. The short linker between the two domains (black) is indicated by an arrow, and the putative gating residues (R156 and E58) are shown in green. (B) Comparison of the proposed gate region for the β-barrel domain of PmOmpA and of EcOmpA. The homologous tetrad of charged sidechains is shown for each protein. (C) Sequence alignment showing the templates used to create the intact model and their secondary structure. The N-terminal template (1BXW) ends with β-strand 8, and the C-terminal template (1R1M) begins with β-strand 9. (For interpretation of the references to colour in this figure legend, the reader is referred to the web version of this article.)

3.1. N-terminal domain model — structural stability

An ensemble of 20 models of the N-terminal domain was generated by Modeller using EcOmpA (pdb code 1BXW) as a template. A model from this ensemble was selected for further investigation by MD simulation on the basis of its stereochemical integrity. The model contained bands of aromatic residues that are situated in ideal positions to interact with the lipid headgroups and help to anchor the protein into the membrane [40,41].

Comparison of the conformational drift of the model of the N-terminal domain from its starting structure relative to other OMP simulations [18,29,42] provides information regarding its relative conformational stability on the timescale of the simulation. Conformational drift was evaluated by calculating the RMSD of the Cα atoms from the initial ($t=0$) structure as a function of time. For Sim1, the all-residue Cα RMSD rose to a plateau of ~3.3 Å at ~2 ns (Table 1). This is higher than the ~1.5 Å observed for the EcOmpA crystal structure [30]. The longer, more flexible extracellular loops of PmOmpA may partially explain this, in particular the amphipathic loop 3 which moves in and out of the lipid bilayer. For the β-barrel Cα atoms the plateau is at ~1.4 Å. This is higher than for the β-barrel Cα RMSD in comparable simulations based on the crystal structure of OmpA (~0.7 Å; [30]) but comparable to that of a homology model of OprF (~1.7 Å; [18]). Further evidence of the stability of the models is provided by DSSP analysis which confirms the integrity of their secondary structure elements throughout the simulation.

Conformational drift of the N-terminal domain in the presence of ~1 M NaCl solution (i.e. Sim2) is lower than the corresponding simulation (Sim1) which contains only neutralising ions, indicating stabilisation of the protein conformation in the presence of an elevated ionic strength.

The residue by residue fluctuations of the simulated structures relative to the average structure provides a measure of the relative flexibility of different regions of the PmOmpA model. The time-averaged root mean square fluctuations (RMSFs) of Cα atoms showed that the greatest flexibility was in the large extracellular loop regions, followed by the intracellular turns, with the β-barrel residues being the least mobile. This is consistent with the predicted topology of the PmOmpA N-terminal domain and is in agreement with simulation studies of EcOmpA [30], of other OMPs [43] and an OMP homology model [18].

Table 2
Water entry into the pore

Simulation	Model	Average 'pore' radius (Å)	Entry of water into 'pore'
Sim1	Barrel	0.16	From both ends of pore to the gate region
Sim2	Barrel, 1 M	0.14	From both ends of pore to the gate region
Sim3	Barrel, uncharged	0.17	From both ends to new gate region
Sim4	Barrel, R156G	0.17	Completely traverses pore

3.2. N-terminal domain model — pore properties

While there is no experimental evidence to suggest pore activity of the N-terminal domain of PmOmpA, its homology with EcOmpA, for which gated pore formation is well documented [44,45], suggests that formation of water filled pores is likely to occur. Molecular dynamics simulations of EcOmpA [29,30] and of its homologue OprF [18] have demonstrated the importance of careful modelling of this domain. The ionisation states of residues facing the barrel interior and salt concentration can affect the stability of the protein/homology model on a simulation timescale. Thus the behaviour of the central 'pore' was analysed in all four simulations (Table 2).

We did not detect any spontaneous water permeation (on a ~10 ns timescale) during either of the wild-type simulations (neutralising salt, and ~1 M NaCl). Whilst water molecules were observed to enter the barrel interior in all the simulations, they did not fully traverse the entire lipid bilayer. Water molecules were observed entering the barrel interior from both sides of the bilayer in simulations of the wild-type model but did not pass a proposed 'gate-region'. This gate-region consisted of a salt-bridge formed between residue E48 and R156. These residues are homologous to the Arg–Glu gating region seen in EcOmpA [29,45], although the gate does not spontaneously open in the current simulations and no waters were observed to pass the constriction during the simulation. However, supporting suggestions for EcOmpA [18,29,30] there is a second glutamate residue (E146) in a position where R156 could hydrogen bond to it instead of to E58, thus 'opening' the gate and allowing water passage. The residue E146 is homologous to the E128 residue observed in EcOmpA (see Fig. 1B).

The ionisation state of E58 was altered (Sim3) so that it was protonated, and would thus disrupt the Arg–Glu salt-bridge. It was hoped that by doing this, the gate-region would be abolished and water passage would occur. As R156 was now no longer interacting with E58 it was free to move and form a new network of hydrogen bonds. Although there were instances of R156 forming the proposed 'open' gate salt-bridge with E146, the gate was effectively closed by E146 also interacting with K93 (homologous to K82 in EcOmpA) that acts as a second gate and prevents water permeation. In the wild-type ionisation state, this second gate region between E146 and K93 could be kept open by the interaction of K93 (EcOmpA K82) with the unprotonated E58 (EcOmpA E52), as proposed by Hong et al. [45]. Finally, a model of the N-terminal domain in which R156 was 'mutated' to a glycine was also constructed and used as the starting point for simulation Sim4. This N-terminal domain was the only simulation that allowed permeation of water, consistent with the suggestion that R156–E58 may form a gate-like region.

3.3. The intact PmOmpA molecule

The model of the intact PmOmpA protein was generated by docking together the homology models of the N-terminal and C-terminal domains (see above for details). The linker region of PmOmpA is comprised of only four residues (in contrast to the

longer and presumably more flexible linker in EcOmpA) and has relatively few degrees of freedom. Therefore manually docking, followed by energy minimisation and checking with PROCHECK, was judged to be a reasonable approach for combining the N-terminal and C-terminal domains. Two simulations of the intact PmOmpA model in a bilayer were performed, at low ionic strength (Sim5) and one in ~1 M NaCl solution (Sim6).

Analysis of the conformational drift provides insights into both the stability of the component domains, and of their movements relative to one another. Thus, in Sim5 the RMSDs of both the N-terminal and C-terminal domains plateau quickly (after ~1.5 ns) to ~2.3 and ~2.9 Å respectively (Fig. 2). Similarly, in Sim6, the RMSD of the N-terminal domain plateaus after ~1.5 ns to a value of ~2.4 Å. In contrast, the C-terminal domain plateaus after 4.5 ns to 4.2 Å, almost twice the RMSD value in Sim5. In both simulations the N-terminal β-barrel is the most stable structural element and plateaus at ~1.3 Å and ~1.25 Å for simulations Sim5 and Sim6 respectively. These results suggest that the domains have stable conformations, which is confirmed through DSSP analysis (data not shown). The secondary structure elements of the whole protein remain stable throughout the simulation. Not only does the linker region (residues 195–200) retain its "random coil" conformation throughout the simulation, but the secondary structure elements around it also retain their integrity.

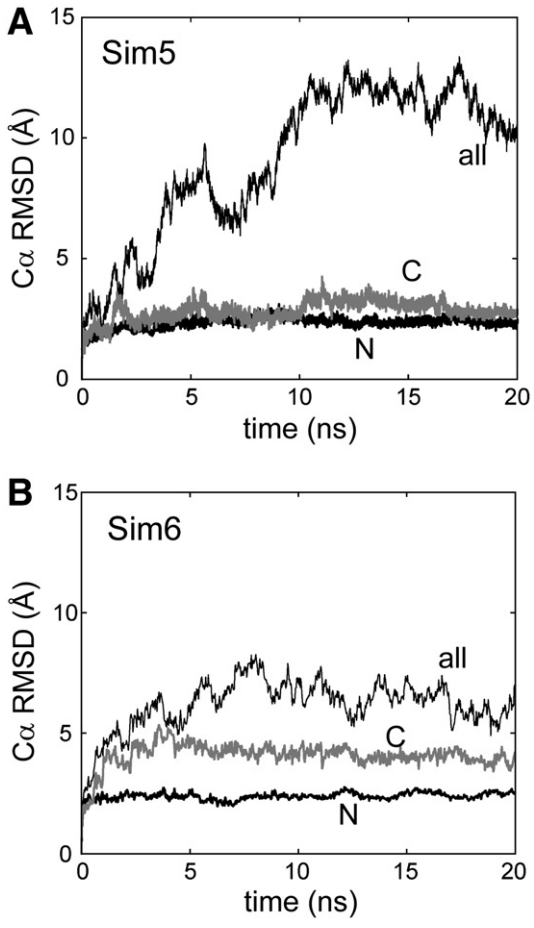

Fig. 2. Conformational drift in simulations of the intact protein, shown as Cα RMSDs from the in initial structures as a function of time for A Sim5 and B Sim6. The Cα RMSDs are shown for all residues (thin black line), and for the N-terminal (thick black line) and C-terminal (thick grey line) domain separately.

In both simulations the RMSD for the whole PmOmpA structure rises to a higher plateau and shows bigger fluctuations than for the two individual domains. In Sim5 the RMSD of the whole molecule reaches a maximum value of ~12 Å from 11 to 17 ns before it finally plateaus at a value of ~10.5 Å, compared to an increase in RMSD for the first 5 ns followed by fluctuations about ~6.5 Å in Sim6. As the RMSDs for the individual domains indicated them to be conformationally stable, the fluctuations in RMSD of the whole molecule indicate significant *inter-domain* motion, which is more pronounced in Sim5. This is confirmed by visualisation of the two simulations (Fig. 3).

The RMSF values for the whole protein are higher than those for each individual domain. The RMSF profile for Sim5 shows a slightly higher average for the C-terminal domain (1.4 Å) compared to the N-terminal domain (1.0 Å), as might be expected for a globular domain relative to a transmembrane β-barrel. The same trend is observed in Sim6, where the C-terminal domain has an average RMSF of 1.3 Å compared to 1 Å for the N-terminal domain. The greatest flexibility is observed for the coil and turn regions in both simulations, the biggest fluctuations overall arise from the C-terminal domain helix 4 which is connected to a flexible loop.

As discussed above, the RMSD of the whole protein is greater than the sum of the two individual domains, suggestive of inter-domain motions (Fig. 3). To decouple the protein motions and identify the most significant ones, we have performed Principal Components Analysis (PCA) on both Sim5 and Sim6 [46,47]. The resulting eigenvectors of the covariance matrix show a substantially bigger contribution of the first eigenvector (44%) to the overall motion of the protein in Sim5, compared to the first eigenvector (20%) in Sim6. In both simulations, the importance of the eigenvectors decays rapidly and only the first four provide significant contributions. "Porcupine" plots [48] provide a convenient static representation of the eigenvectors enabling their visualisation. From such analysis it can be seen that (Fig. 4) in Sim5 the C-terminal domain moves relative to the N-terminal domain and to the inner leaflet of the bilayer, whereas in Sim6 the most important motion is a 'twisting' of both domains.

3.4. Lipid/potein interactions

In order to further evaluate the intact PmOmpA model with respect to the differences in the movement of the C-terminal domain with respect to transmembrane domain and the lipid bilayer, we have analysed the lipid–protein interactions in Sim5 and Sim6. Recent MD studies have shown simulations of ~10 ns to provide insights into the lipid–protein interactions of a number of membrane proteins [41]. We evaluated the total number of lipid–protein interactions (defined by a lipid–protein distance cutoff of 3.5 Å) as a function of time (Fig. 5A). In Sim5

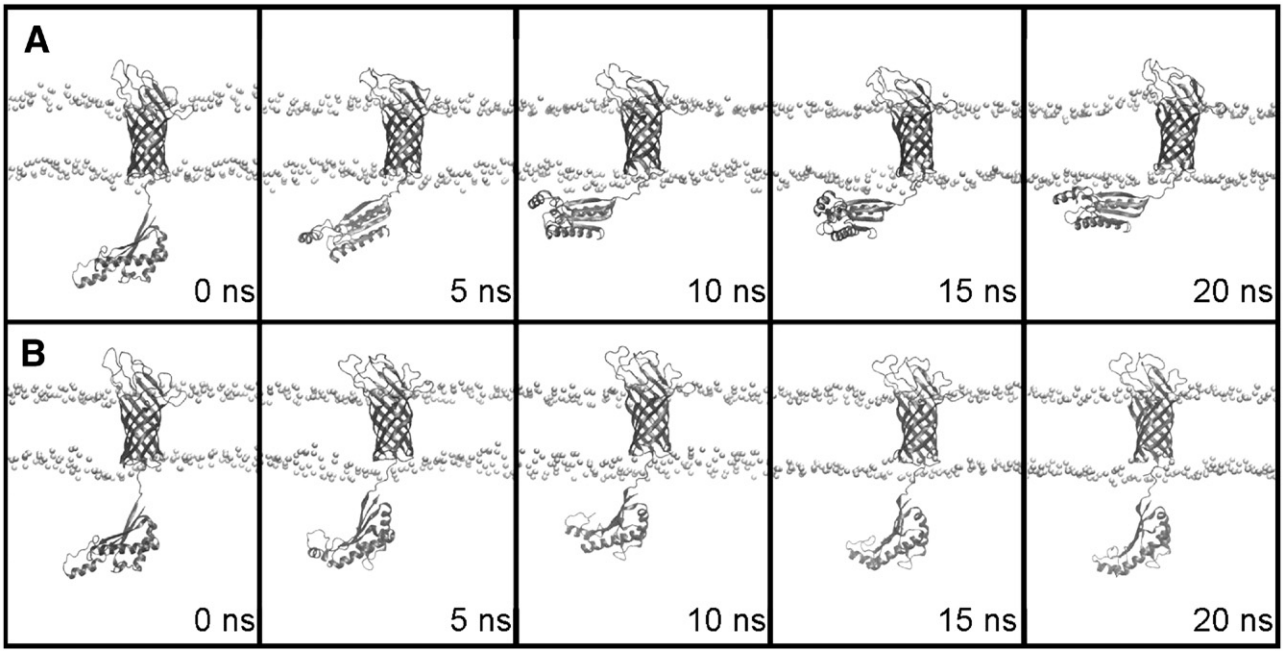

Fig. 3. Snapshots of structures from A Sim5 and B Sim6 every 5 ns, showing the protein and the bilayer (the latter represented by the P atoms of the lipid headgroups).

the total number of interactions between the protein and the lipids increases significantly over the course of the simulation and plateaus at ~520 interactions over the last 4 ns. In particular, the increase in number of interactions after ~9 ns is largely due to the C-terminal domain interacting with the inner leaflet of the lipid bilayer. In contrast, for Sim6 the number of interactions rises over the first ~10 ns after which it fluctuates. Thus there is a marked difference in the pattern of the interactions for the two simulations. Similar trends in lipid–protein interactions were observed in Sim7 and Sim8, in which the intact PmOmpA was embedded in a DMPE lipid bilayer. These simulations were started by saving coordinates from Sim5 (at t=6 ns for Sim7 and t=20 ns for Sim8). The PC lipid headgroups were then converted to PE headgroups. After 25 ns in Sim7 and 20 ns in Sim8, in both simulations the total number of lipid–protein interactions was ~550 which is comparable to the value of ~520 observed for Sim5 (comparing Fig. 5A and Fig. 5B).

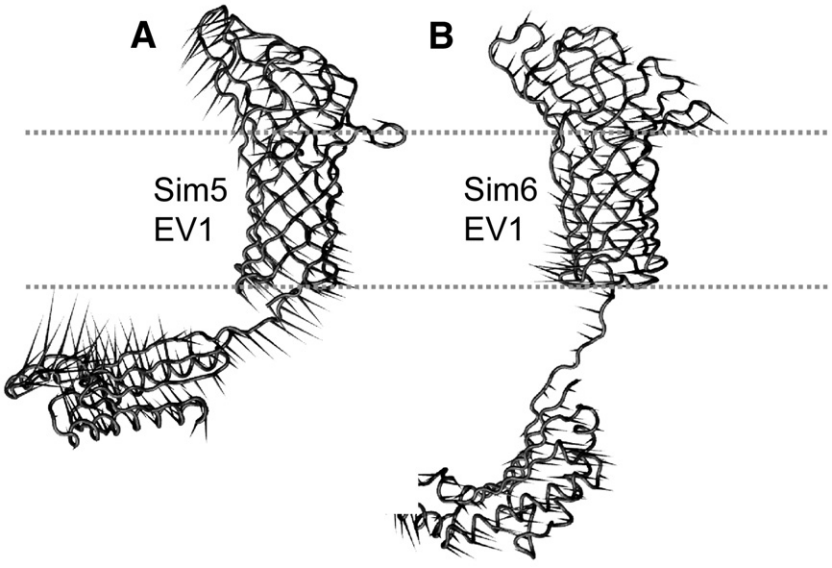

Fig. 4. Eigenvector 1 for simulations Sim5 (left) and Sim6 (right) shown as 'porcupine' plot in which the displacement of each Cα atom is indicated by a cone. The approximate position of the bilayer is indicated for reference by the horizontal lines. Sim5 and Sim6 both show some movement of the extracellular loops, and tilting of the β-barrel in the membrane. However, whereas Sim5 indicates the primary movement of the C-terminal domain is towards the membrane, Sim6 indicates a small twisting movement dominates the C-terminal domain dynamics.

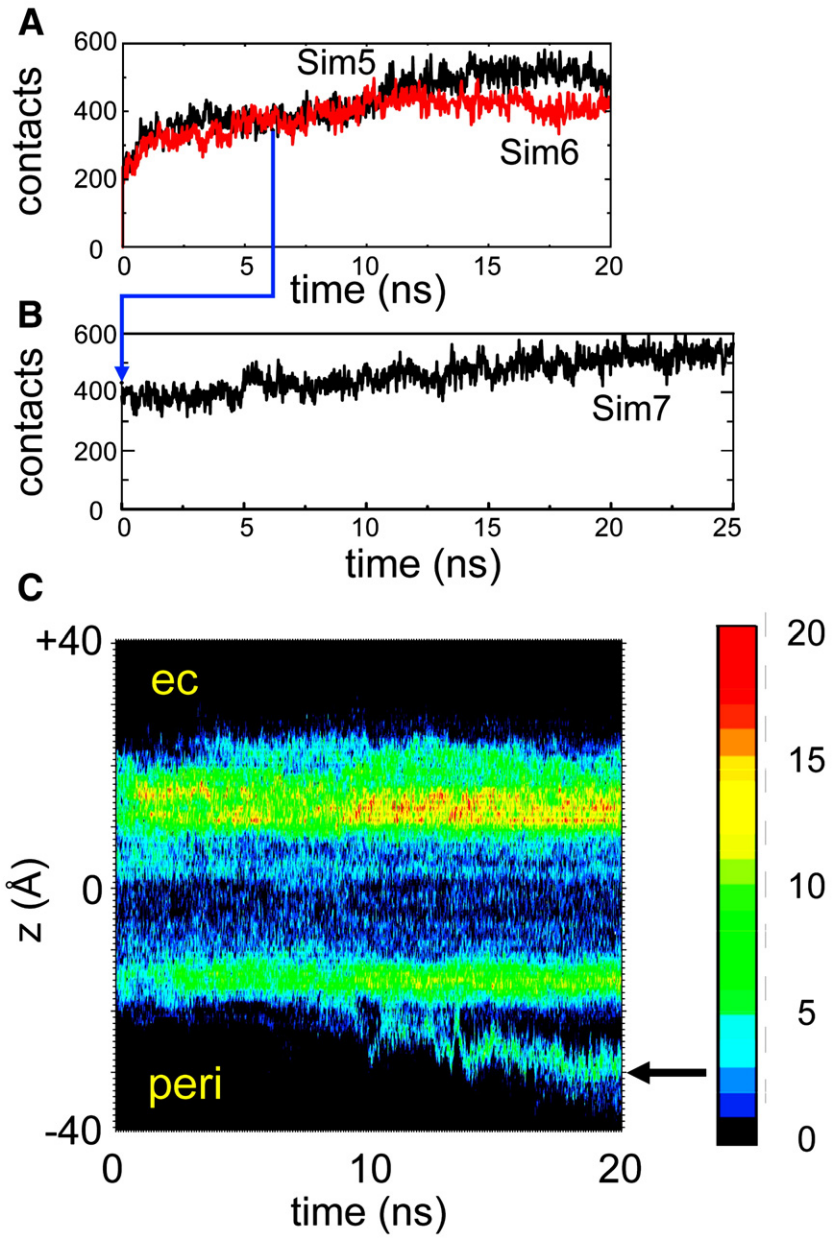

Fig. 5. (A) Total number of protein/lipid contacts (cutoff distance 3.5 Å) as a function of time for Sim5 (black) and Sim6 (red). (B) Total number of protein/lipid contacts for Sim7, with PmOmpA in a DMPE bilayer. The starting conformation of the simulation is taken from $t=6$ ns in Sim5. (C) Number of protein/lipid contacts for Sim5 shown as a function of position along the bilayer normal (z) and time. The arrow indicates the region of the graph corresponding to contacts formed between the C-terminal domain and phospholipid headgroups. (For interpretation of the references to colour in this figure legend, the reader is referred to the web version of this article.)

The contrasting pattern of lipid–protein interactions at low and high ionic strength is a direct consequence of the behaviour of the C-terminal domain. If we consider just the N-terminal domain and the lipid head groups then the number of lipid–protein interactions fluctuates about ~180 in Sim5 compared with ~175 in Sim6. These values are comparable to the values reported for the N-terminal domain homology model of OprF [18] suggesting conservation of overall lipid–protein interactions between homologues. Similar levels of lipid/protein interaction have been observed experimentally for EcOmpA [49] providing us with further confidence in our model of PmOmpA.

The time dependence and nature of the lipid–protein (both domains) interactions were monitored by further analysing the number of interactions as a function of position along the bilayer normal and of time. In both simulations, two distinct 'bands' of interactions corresponding to the head group regions of the bilayer were evident. The bands were more pronounced for the extracellular leaflet i.e. the PmOmpA N-terminal barrel makes more contacts to the outer lipid leaflet compared to the inner leaflet. The β-barrel has large extracellular loops that can interact with the outer leaflet, whilst there is less chance of the small intracellular turns making extensive contacts with the inner leaflet.

A third band of interactions is observed on the periplasmic side of the lipid bilayer in Sim5. This band corresponds to the interactions of the C-terminal domain. The absence of such a third band from Sim6 reflects the lack of movement of the C-terminal domain towards the lipid bilayer in this simulation.

To understand the reasons for the movement of the C-terminal domain towards the bilayer in Sim5 and the contrasting lack of movement in Sim6, we have considered the interactions with lipid tails and head groups separately. It is apparent that the majority of the C-terminal contacts with the lipid bilayer arise from charged and polar residues interacting with the lipid head groups (Fig. 6). In fact, of the ten C-terminal domain residues that interact most with lipids during Sim5 (namely E201, T206, E236, V199, Q239, D316, S204, K205, R319, E321), six are charged. Similarly, in Sim7 and Sim8 (DMPE) the residues forming most of the interactions with lipids also include E201, E236, and K205. Thus the interactions of the C-terminal domain with the bilayer are largely electrostatic. In the presence of 1 M NaCl, the charges on the lipid head groups and charged protein residues are shielded by the Na^+ and Cl^- ions. This results in a reduced electrostatic attraction between the lipid head groups and the C-terminal domain and therefore there is less C-terminal domain movement towards the bilayer in Sim6.

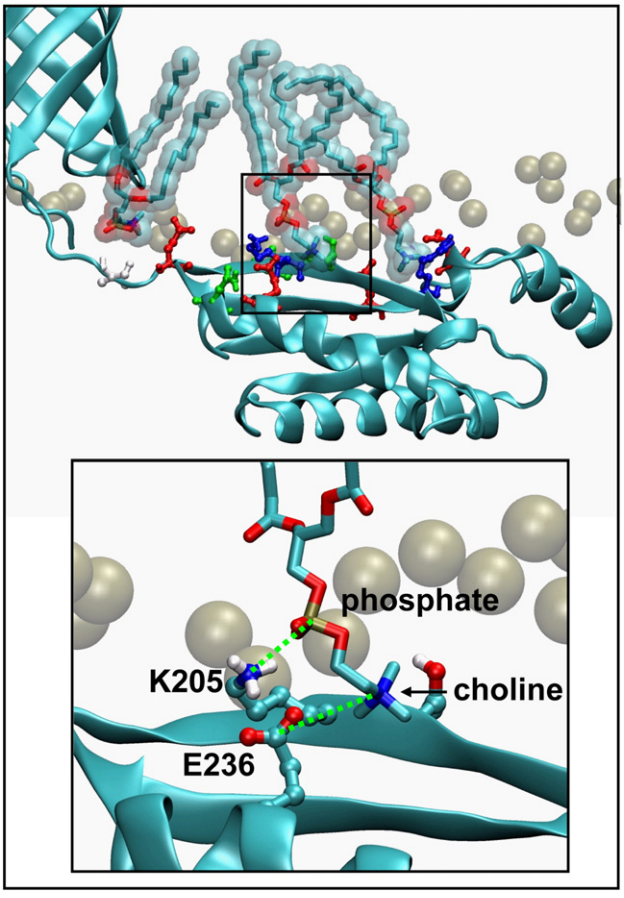

Fig. 6. A sample structure from the end of Sim5 illustrating the electrostatic interactions between the lipid headgroups and residues of the C-terminal domain. In the insert, examples of the types of electrostatic interactions (green broken lines) between K205 and a lipid phosphate, and between E236 and the choline of the same lipid molecule are highlighted. The residues K205 and E236 were also found to contact the membrane in Sim7 and Sim8.

4. Discussion

The simulation results indicate that the N-terminal β-barrel domain of PmOmpA exhibits similar conformational dynamics to e.g. the N-terminal domain of EcOmpA, and to the homologous domain of OprF in *P. aeruginosa*. This suggests that the overall conformational dynamic properties may be shared with other homologous 8-stranded OMP domains, e.g. those of OmpX [50,51], PagP [10,11], and NspA [52]. Specifically, the β-barrel is conformationally stable, and does not fluctuate appreciably on a ~20 ns timescale in the presence of 1 M NaCl. The large extracellular loop regions are significantly more flexible and this is enhanced under lower ionic strength conditions.

Our homology model of the intact PmOmpA protein (i.e. the N- terminal+C-terminal domains) is also stable in a DMPC lipid bilayer over a 20-ns timescale. Encouragingly, the secondary structure of the entire model is retained throughout both simulations. Under low salt conditions (only neutralising counter ions present), motion of the C-terminal domain towards the lipid bilayer, until it is in contact with the lipid head groups, is observed. This degree of flexibility is perhaps somewhat surprising given the short length (4 residues) of the linker region. Decomposition of the lipid–protein interactions under low salt conditions in both DMPC and DMPE bilayers has shown that these interactions are dominated by electrostatic attraction. In 1 M NaCl, these long-range forces of attraction are shielded, reducing interactions of the surface of the C- terminal domain with the polar lipid head groups. This suggests that interactions of extra-membrane domains of OMPs with bilayers may be rather complex and modulated by local environmental conditions. Interestingly, even with the relatively short inter-domain region in PmOmpA, the link between the TM domain and the C-terminal peptidoglycan binding domain is relatively flexible. This may be of possible functional significance in enabling coupling of the OM to the peptidoglycan matrix whilst allowing for variations in the exact membrane/peptidoglycan distance.

Of course, this analysis assumes that the structure of an intact OmpA protein may be modelled from the structures of isolated N-terminal and C-terminal domains. Given the nature of the domains this seems likely. One should also allow for the possibility of refolding to give a single, larger TM domain for the intact OmpA [53]. However, recent studies of gene duplication constructs of the related protein OmpX [54] suggest that the β-barrel is an independent folding unit, and so support the assumption underlying the modelling of intact PmOmpA.

It is also important to consider the methodological limitations of the current studies. The primary limitation of the simulations *per se* is the relatively short duration (10 to 20 ns) of the MD simulations. Longer simulations would improve the sampling of the conformational dynamics [55,56]. However, to some extent we have addressed this by performing multiple simulations. From the perspective of the simulation system the

major approximation is the use of a simple DMPC bilayer. A closer approximation to in vivo would be to use an OM model including lipopolysaccharide [57], and possibly also the periplasmic peptidoglycan layer [58]. However, despite these limitations, the current study is encouraging in that it provides evidence that computational approaches may be applied to more complex, multi-domain OMPs, rather than just to TM β-barrels. In combination with recent developments in sequence-based modelling of OMP TM architectures [23], this suggests that we are making significant progress towards *in silico* proteomics of OMPs.

Acknowledgments

This work was supported by grants from the BBSRC and EPSRC (as part of the Bionanotechnology IRC) and the Wellcome Trust. TC is a BBSRC research student.

References

[1] M.P. Molloy, B.R. Herbert, M.B. Slade, T. Rabilloud, A.S. Nouwens, K.L. Williams, A.A. Gooley, Proteomic analysis of the *Escherichia coli* outer membrane, Eur. J. Biochem. 267 (2000) 2871–2881.
[2] W.C. Wimley, Toward genomic identification of β-barrel membrane proteins: composition and architecture of known structures, Prot. Sci. 11 (2002) 301–312.
[3] U. Baumann, E. Mansouri, B.U. von Specht, Recombinant OprF–OprI as a vaccine against *Pseudomonas aeruginosa* infections, Vaccine 22 (2004) 840–847.
[4] S. Worgall, M. Rivara, A. Krause, N.R. Hackett, P.W. Rovelink, J.T. Bruder, T.J. Wickham, I. Kovesdi, R.G. Crystal, Protection against pulmonary infection with *P. aeruginosa* following immunization with an adenovirus vector expressing a *P. aeruginosa* OprF epitope, Molec. Ther. 9 (2004) 689.
[5] L.K. Tamm, A. Arora, J.H. Kleinschmidt, Structure and assembly of beta-barrel membrane proteins, J. Biol. Chem. 276 (2001) 32399–32402.
[6] R. Koebnik, K.P. Locher, P. Van Gelder, Structure and function of bacterial outer membrane proteins: barrels in a nutshell, Mol. Microbiol. 37 (2000) 239–253.
[7] S.W. Cowan, T. Schirmer, G. Rummel, M. Steiert, R. Ghosh, R.A. Pauptit, J.N. Jansonius, J.P. Rosenbusch, Crystal structures explain functional properties of two *E. coli* porins, Nature 358 (1992) 727–733.
[8] J.D. Faraldo-Gómez, M.S.P. Sansom, Acquisition of siderophores in gram-negative bacteria, Nat. Rev., Mol. Cell Biol. 4 (2003) 105–115.
[9] A. Pautsch, G.E. Schulz, Structure of the outer membrane protein A transmembrane domain, Nat. Struct. Biol. 5 (1998) 1013–1017.
[10] P.M. Hwang, W.Y. Choy, E.I. Lo, L. Chen, J.D. Forman-Kay, C.R.H. Raetz, G.G. Privé, R.E. Bishop, L.E. Kay, Solution structure and dynamics of the outer membrane enzyme PagP by NMR, Proc. Natl. Acad. Sci. U. S. A. 99 (2002) 13560–13565.
[11] V.E. Ahn, E.I. Lo, C.K. Engel, L. Chen, P.M. Hwang, L.E. Kay, R.E. Bishop, G.G. Privé, A hydrocarbon ruler measures palmitate in the enzymatic acylation of endotoxin, EMBO J. 23 (2004) 2931–2941.
[12] S.M. Prince, M. Achtman, J.P. Derrick, Crystal structure of the OpcA integral membrane adhesin from *Neisseria meningitides*, Proc. Natl. Acad. Sci. U. S. A. 99 (2002) 3417–3421.
[13] A. Pautsch, G.E. Schulz, High-resolution structure of the OmpA membrane domain, J. Mol. Biol. 298 (2000) 273–282.
[14] R. Orme, C.W.I. Douglas, S. Rimmer, M. Webb, Proteomic analysis of *Escherichia coli* biofilms reveals the overexpression of the outer membrane protein OmpA, Proteomics 6 (2006) 4269–4277.
[15] S. Grizot, S.K. Buchanan, Structure of the OmpA-like domain of RmpM from *Neisseria meningitidis*, Mol. Microbiol. 51 (2004) 1027–1037.
[16] A. Arora, F. Abildgaard, J.H. Bushweller, L.K. Tamm, Structure of outer membrane protein A transmembrane domain by NMR spectroscopy, Nat. Struct. Biol. 8 (2001) 334–338.
[17] S.M. Dabo, A.W. Confer, R.A. Quijano-Blas, Molecular and immunological characterization of *Pasteurella multocida* serotype A : 3 OmpA: evidence of its role in *P. multocida* interaction with extracellular matrix molecules, Microb. Pathogen. 35 (2003) 147–157.
[18] S. Khalid, P.J. Bond, S.S. Deol, M.S.P. Sansom, Modelling and simulations of a bacterial outer membrane protein: OprF from *Pseudomonas aeruginosa*, Proteins: Struct. Funct. Bioinf. 63 (2005) 6–15.
[19] J.S. Oakhill, B.J. Sutton, A.R. Gorringe, R.W. Evans, Homology modelling of transferrin-binding protein A from *Neisseria meningitidis*, Prot. Engng. Des. Sel. 18 (2005) 221–228.
[20] F.S. Berven, K. Flikka, H.B. Jensen, I. Eidhammer, BOMP: a program to predict integral β-barrel outer membrane proteins encoded within genomes of Gram-negative bacteria, Nucleic Acids Res. 32 (2004) W394–W399.
[21] P.J. Bond, M.S.P. Sansom, The simulation approach to bacterial outer membrane proteins, Mol. Memb. Biol. 21 (2004) 151–162.
[22] T. Lazaridis, Structural determinants of transmembrane beta-barrels, J. Chem. Theory Comp. 1 (2005) 716–722.
[23] J. Waldispuhl, B. Berger, P. Clote, J.M. Steyaert, Predicting transmembrane beta-barrels and interstrand residue interactions from sequence, Proteins Struct. Funct. Bioinf. 65 (2006) 61–74.
[24] J.D. Thompson, D.G. Higgins, T.J. Gibson, CLUSTAL W: improving the sensitivity of progressive multiple sequence alignment through sequence weighting, position-specific gap penalties and weight matrix choice, Nucleic Acids Res. 22 (1994) 4673–4680.
[25] R. Chenna, H. Sugawara, T. Koike, R. Lopez, T.J. Gibson, D.G. Higgins, J.D. Thompson, Multiple sequence alignment with the Clustal series of programs, Nucleic Acids Res. 31 (2003) 3497–3500.
[26] A. Sali, T.L. Blundell, Comparative protein modeling by satisfaction of spatial restraints, J. Mol. Biol. 234 (1993) 779–815.
[27] R. Sanchez, A. Sali, Comparative protein structure modeling. Introduction and practical examples with modeller, Methods Mol. Biol. 143 (2000) 97–129.
[28] R.A. Laskowski, M.W. Macarthur, D.S. Moss, J.M. Thornton, Procheck — a program to check the stereochemical quality of protein structures, J. Appl. Crystallogr. 26 (1993) 283–291.
[29] P.J. Bond, J.D. Faraldo-Gómez, M.S.P. Sansom, OmpA — A pore or not a pore? Simulation and modelling studies, Biophys. J. 83 (2002) 763–775.
[30] P.J. Bond, M.S.P. Sansom, Membrane protein dynamics vs. environment: simulations of OmpA in a micelle and in a bilayer, J. Mol. Biol. 329 (2003) 1035–1053.
[31] E. Lindahl, B. Hess, D. van der Spoel, GROMACS 3.0: a package for molecular simulation and trajectory analysis, J. Molec. Model 7 (2001) 306–317.
[32] W.R.P. Scott, P.H. Hunenberger, I.G. Tironi, A.E. Mark, S.R. Billeter, J. Fennen, A.E. Torda, T. Huber, P. Kruger, W.F. van Gunsteren, The GROMOS biomolecular simulation program package, J. Phys. Chem., A 103 (1999) 3596–3607.
[33] T. Darden, D. York, L. Pedersen, Particle mesh Ewald — an N.log(N) method for Ewald sums in large systems, J. Chem. Phys. 98 (1993) 10089–10092.
[34] H.J.C. Berendsen, J.P.M. Postma, W.F. van Gunsteren, A. DiNola, J.R. Haak, Molecular dynamics with coupling to an external bath, J. Chem. Phys. 81 (1984) 3684–3690.
[35] M. Parrinello, A. Rahman, Polymorphic transitions in single-crystals — a new molecular-dynamics method, J. Appl. Phys. 52 (1981) 7182–7190.
[36] B. Hess, H. Bekker, H.J.C. Berendsen, J.G.E.M. Fraaije, LINCS: a linear constraint solver for molecular simulations, J. Comp. Chem. 18 (1997) 1463–1472.
[37] W. Kabsch, C. Sander, Dictionary of protein secondary structure: pattern-recognition of hydrogen-bonded and geometrical features, Biopolymers 22 (1983) 2577–2637.
[38] O.S. Smart, J.G. Neduvelil, X. Wang, B.A. Wallace, M.S.P. Sansom, Hole: a program for the analysis of the pore dimensions of ion channel structural models, J. Mol. Graph. 14 (1996) 354–360.
[39] W. Humphrey, A. Dalke, K. Schulten, VMD — visual molecular dynamics, J. Mol. Graph. 14 (1996) 33–38.

[40] J.A. Killian, G. von Heijne, How proteins adapt to a membrane–water interface, Trends Biochem. Sci. 25 (2000) 429–434.
[41] S.S. Deol, P.J. Bond, C. Domene, M.S.P. Sansom, Lipid–protein interactions of integral membrane proteins: a comparative simulation study, Biophys. J. 87 (2004) 3737–3749.
[42] S. Khalid, M.S.P. Sansom, Molecular dynamics simulations of a bacterial autotransporter: NalP from *Neisseria meningitidis*, Mol. Membr. Biol. 23 (2006) 499–508.
[43] D.P. Tieleman, H.J.C. Berendsen, A molecular dynamics study of the pores formed by *Escherichia coli* OmpF porin in a fully hydrated palmitoyloleoylphosphatidylcholine bilayer, Biophys. J. 74 (1998) 2786–2801.
[44] A. Arora, D. Rinehart, G. Szabo, L.K. Tamm, Refolded outer membrane protein A of *Escherichia coli* forms ion channels with two conductance states in planar lipid bilayers, J. Biol. Chem. 275 (2000) 1594–1600.
[45] H. Hong, G. Szabo, L.K. Tamm, Electrostatic couplings in OmpA ion-channel gating suggest a mechanism for pore opening, Nat. Chem. Biol. 2 (2006) 627–635.
[46] A.E. Garcia, Large-amplitude nonlinear motions in proteins, Phys. Rev. Lett. 68 (1992) 2696–2699.
[47] A. Amadei, A.B.M. Linssen, H.J.C. Berendsen, Essential dynamics of proteins, Proteins, Struct. Funct. Genet. 17 (1993) 412–425.
[48] K. Tai, T. Shen, U. Börjesson, M. Philippopoulos, J.A. McCammon, Analysis of a 10-ns molecular dynamics simulation of mouse acetylcholinesterase, Biophys. J. 81 (2001) 715–724.
[49] M. Ramakrishnan, C.L. Pocanschi, J.H. Kleinschmidt, D. Marsh, Association of spin-labeled lipids with β-barrel proteins from the outer membrane of *Escherichia coli*, Biochem. 43 (2004) 11630–11636.
[50] C. Fernandez, C. Hilty, G. Wider, P. Güntert, K. Wüthrich, NMR structure of the integral membrane protein OmpX, J. Mol. Biol. 336 (2004) 1211–1221.
[51] R.A. Böckmann, A. Caflisch, Spontaneous formation of detergent micelles around the outer membrane protein OmpX, Biophys. J. 86 (2005) 3191–3204.
[52] L. Vandeputte-Rutten, M.P. Bos, J. Tommassen, P. Gros, Crystal structure of Neisserial Surface Protein A (NspA), a conserved outer membrane protein with vaccine potential, J. Biol. Chem. 278 (2003) 24825–24830.
[53] E. Zakharian, R.N. Reusch, Kinetics of folding of *Escherichia coli* OmpA from narrow to large pore conformation in a planar bilayer, Biochem. 44 (2005) 6701–6707.
[54] T. Arnold, M. Poynor, S. Nussberger, A.N. Lupas, D. Linke, Gene duplication of the eight-stranded β-barrel OmpX produces a functional pore: a scenario for the evolution of transmembrane β-barrels, J. Mol. Biol. 366 (2007) 1174–1184.
[55] J.D. Faraldo-Gómez, L.R. Forrest, M. Baaden, P.J. Bond, C. Domene, G. Patargias, J. Cuthbertson, M.S.P. Sansom, Conformational sampling and dynamics of membrane proteins from 10-nanosecond computer simulations, Proteins, Struct., Funct., Bioinf. 57 (2004) 783–791.
[56] A. Grossfield, S.E. Feller, M.C. Pitman, Convergence of molecular dynamics simulations of membrane proteins, Proteins, Struct. Func. Bioinf. 67 (2007) 31–40.
[57] R.D. Lins, T.P. Straatsma, Computer simulation of the rough lipopolysaccharide membrane of *Pseudomonas aeruginosa*, Biophys. J. 81 (2001) 1037–1046.
[58] D. Pink, J. Moeller, B. Quinn, M. Jericho, T. Beveridge, On the architecture of the Gram-negative bacterial murein sacculus, J. Bacteriol. 182 (2000) 5925–5930.